Full-color nanorouter for high-resolution imaging

Mingjie Chen[1,#], Long Wen[1,#], Dahui Pan[1], David R. S. Cumming[2], Xianguang Yang[1,*] and Qin Chen[1,*]

[1]Institute of Nanophotonics, Jinan University, Guangzhou 511443, China

[2]James Watt School of Engineering, University of Glasgow, Glasgow G12 8QQ, UK

[*]chenqin2018@jnu.edu.cn, xianguang@jnu.edu.cn

[#]equal contribution

Abstract

Pixel scaling effects have been a major issue for the development of high-resolution color image sensors due to the reduced photoelectric signal and the color crosstalk. Various structural color techniques have been proposed and demonstrated the large freedom in color manipulation by the structure design. However, the optical efficiency and the color distortion limit the practical applications due to its intrinsic filtering mechanism. Instead, on-chip full-color routing is quite charming for improving the signal-to-noise ratio. In this paper, a single-layer quick response code like nanorouter is proposed for the full-color light routing in a pixel level of image sensors. It shows much higher routing efficiency than various planar lens schemes for signal wavelength focusing. Moreover, over 60% signal enhancement with robust polarization insensitivity is obtained in all three primary color bands with a same nanorouter by a multi-objective optimization method. Negligible color distortion is observed from the reconstructed color image. Such a simple nanorouter scheme is promising for the development of image sensor, photovoltaics and display.

Since the film camera was replaced to the digital camera, it has been a main trend to pursue small pixel sizes entering into a sub-micron scale to meet the requirement of high-resolution imaging [1, 2]. The shrinkage of the pixel size of ISs raises serious signal-to-noise issues and brings challenges to conventional optical components [3]. Many attempts have been recently made to design structural color filters that applying various nano-optical effects, including extraordinary transmission (EOT) [4], metallic nanoantennas [5], Fano resonance [6], Mie resonance [7], guided mode resonance (GMR) [8], and so on. Compared to the conventional dye color filters based on material absorption, structural color techniques realize spectral filtering via artificial micro-/nano-structures with the advantages of complementary metal-oxide-semiconductor (CMOS) process compatibility, stability and suppressed spatial color crosstalk [9]. Although thorough investigation has been made to explore the fundamental physics [10], grow high-quality materials [11] and optimize the fabrication and integration methods [12] of structural color techniques, none could beat dye color filters in terms of light transmission efficiency (~90%) and color purity [13]. In addition, most structural color filters are based on periodic nanostructures and show an obvious dependence of the filtering performance on the period number [7, 9, 14]. Serious degeneration involving both optical efficiency and color purity occurs with the reducing period number for fitting in a single pixel. Therefore, it is important to find out the intrinsic limitation of the optical efficiency and put forward a new technique route to address this issue.

In current color imaging or display systems, illumination light is usually divided into several parts in each unit cell according to the spatial distribution of pixels, for example, four pixels in a Bayer array with a *R-G-G-B* unit cell [15] or three pixels in a *R-G-B* unit cell [16]. In each pixel, light in one color band transmits through a color filter and is detected by a photodiode or human eyes. Obviously, in such a configuration most light is filtered out without any contribution to the photoelectric or photobiological signal. For example, approximately one third light component is detected but two thirds are wasted in a *R-G-B* unit cell as shown in Figure 1(a), i.e., a maximum optical efficiency is only 33% even if the color filter has transmittance as high as 100%. In contrast, routing light to appropriate directions determined by its wavelength rather than excluding the unwanted light components by the filters is expected to provide higher optical efficiencies as shown in Figure 1(b) [17]. Traditionally, diffractive gratings are widely used to direct multiwavelength light to different spatial positions. However, its bulky size limits its applications in ISs. Plasmonic antennas have shown the color sorting functions in a subwavelength

scale [18]. However, the intrinsic high loss of metallic nanostructures limits the overall optical efficiency for imaging applications. Dielectric metasurfaces allow remarkable optical manipulation with extremely low loss [19-21]. A full-color router was reported with a GaN metalens, where multiwavelength routing was realized by integrating 4×4 spatial multiplex nanopillars into a complex unit cell [20]. However, the router has a dimension of 50 μm × 50 μm with a focal length of 110 μm, which is not appropriate for the integration in ISs. Moreover, the routing efficiencies of *R*, *G* and *B* colors drop to 15-38% as a cost of multiplexing. Scattering by dielectric nanoantennas has also been explored for color routing [17,22]. However, they usually suffer from large spectral crosstalk because only a part of pixels are covered with antennas, i.e. the overall improvement of the detected light power mainly comes from the nonselective light transmission in those white (*W*) pixels. For example, the normalized light transmission of the *G* pixel is less than 1 without any enhancement [17]. Recently, a gradient-based optimization approach was used in the color nanorouter design and showed excellent wavelength-dependent spatial light sorting [23-25]. However, a two-dimensional (2D) model cannot reveal the actual physics and directly instruct the practical device design [25]. Both a design element of 10 nm×10 nm and the 3D porous structures in a nanoscale are far beyond the fabrication capability of current standard IS processes [24, 25].

In this paper, we proposed quick response (QR) code like full-color nanorouters of high optical efficiency and high color purity for the applications in ISs with a micron-scale pixel size. Such single-layer color nanorouters consist of titanium oxide nanoblocks in a QR-code like array in a low refractive index environment on the surface of a monochrome IS, which is easy to fabricate and compatible to the CMOS processes. Full-color routing with low polarization dependence was demonstrated in a 1.1 μm×1.1 μm-pixel IS with an improvement of 2.88 times of the total detected power in a unit cell, where an average optical efficiency of each pixel is enhanced by a factor of 1.66 with a color quality of 0.63. Moreover, 30% improvement on optical efficiency together with a color quality as good as the dye color filters are also demonstrated. The reconstructed image from a standard multispectral image shows excellent color fidelity and obvious improvement of brightness.

A single-layer QR-code like nanorouter consisting of high refractive index nanoblocks in a QR-code like array in a low refractive index environment is proposed as shown in Figure 1c. Instead of the commonly used *R*-*G*-*G*-*B* unit cell in a Bayer array in most image sensors, a *R*-*G*-*B* unit cell as shown in Figure 1b is adopted because a large duty cycle of G pixel won't increase the flux ratio of green color in

a spectral routing scheme. The nanorouter is optimized by an algorithm of NSGA-II, which has advantages in multi-objective optimization [26]. Nanoblocks distribute inside each pixel in an area of 1.1×1.1 μm^2, where each block has a lateral dimension of 100 nm×100 nm for a feasible design considering current fabrication capability. The block distribution is different in *R*, *G* and *B* pixels but the distribution in each unit cell repeats over the whole pixel array.

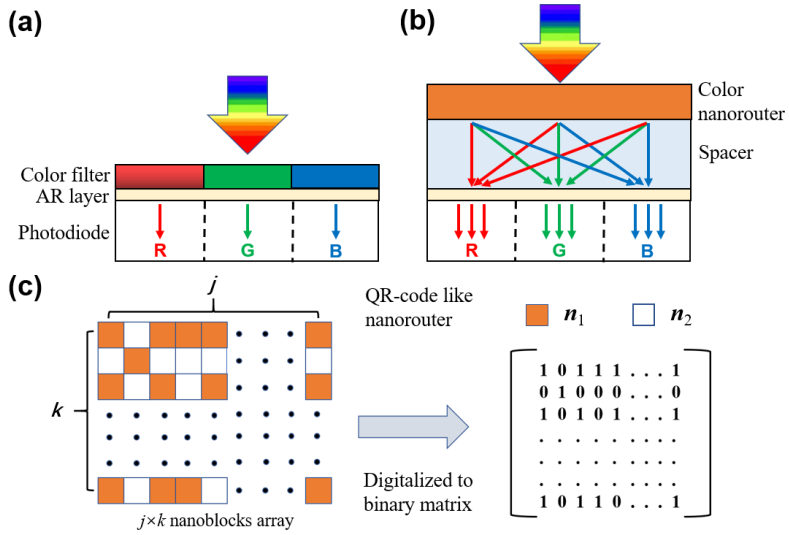

Figure 1. Schematic of spectral engineering in an IS. (a) An IS with color filters. (b) An IS with color nanorouters. (c) Schematic of a QR-code like color nanorouter.

Nanorouters for *G* color were first designed based on the above method as shown in Figure 2 (Supporting information, S1), where the nanorouters cover three pixels and are expected to sort the green light incident on the whole unit cell to the middle pixel. Optical efficiency of the nanorouter for sorting green light to the middle pixel is defined as the ratio of the collected flux of the middle pixel to the incident flux over the unit cell (three pixels) at a wavelength of 550 nm. For the conventional dye filter scheme, the maximum efficiency is 30% assuming 90% transmittance of the dye filter. In contrast, the nanorouter are able to collect the incident light on the neighboring pixels to the middle pixel as an antenna resulting in an improved optical efficiency. As shown in Figure 2b, the improvement is quite robust to the spacer thickness with an enhancement factor between 2.4-2.8 times compared to the color filtering scheme based on the dye filters. The light routing phenomenon is clearly seen from the electric field distribution in Figure 2c. At the surface of the silicon diode, the electric field is concentrated inside the middle pixel as expected with weak crosstalk to the other two pixels. The relatively uniform electric field at the top surface of nanorouters gradually concentrates to the middle pixel in both vertical and lateral directions. This promising result demonstrates a remarkable improvement of optical efficiency of the

color routing scheme over the color filtering scheme, which is a key point in the further development of super-resolution ISs. It is interesting to compare the optimization results of the proposed structure to the ones based on the fundamental optical principles such as dielectric planar lens with propagation phase [28], metalens with geometric phase [27] and plasmonic flat lens with resonant phase [29]. All these planar lens designs have the same lateral size of 3.3 μm×1.1 μm as the nanorouters (Supporting information, S2). As seen from Figure 2c, all lenses show light focusing but the electric field intensity at the focuses are much weaker than the nanorouters. The optical efficiency of nanorouters, lenses with propagation phase, geometric phase and resonance phase is 83.8%, 67.6%, 72.9% and 14.6% respectively. It is attributed to the limited numerical aperture (NA) due to the small lateral size of the lenses [30]. The coarse phase distribution and sparse light channels limited by the feature size of the nanostructures in a fixed NA also reduces the interference at the right focus. In contrast, the GA algorithm generated design shows a more robust light routing.

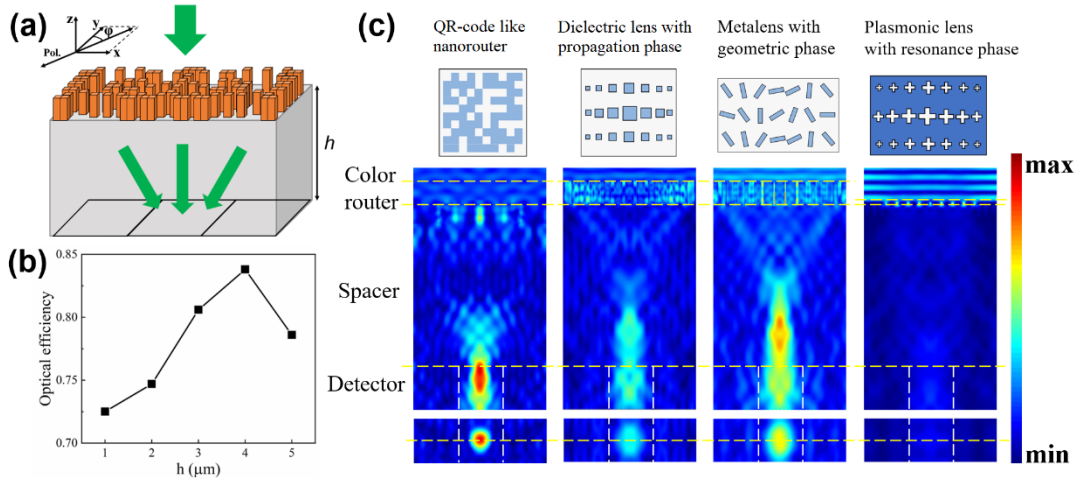

Figure 2. (a) Schematic of a nanorouter for *G* color in an IS with a *RGB* unit cell. (b) Optical efficiencies at different spacer thicknesses at a wavelength of 550 nm with *y*-polarized normal incidence. (c) Cross-section electric field distributions of a QR-code like nanorouter, dielectric lens with propagation phase, metalens with geometric phase and plasmonic lens with resonant phase. The thickness of spacer *h* is set to 4 μm. Yellow lines indicate the positions of nanostructures, spacers and detectors. White dashed lines indicate the position of each pixel.

For full-color imaging in practical applications, a multi-wavelength router is required to enhance the optical efficiency in each color band. Sectoring and interleaving are the two main approaches used to design multi-wavelength or multifunctional metasurfaces [23]. However, the optical efficiencies of the multiplexed structure were found to drop significantly due to the reduced aperture or the crosstalk [20]. In contrast, the algorithm assisted design including the gradient inverse method and the GA method has a large design freedom to balance the choices of multiple dimensional parameters and intrinsically

involve all the potential physical effects including the coupling between nanostructures and the aperture influence. Therefore, it will be more efficient for a multi-objective optimization.

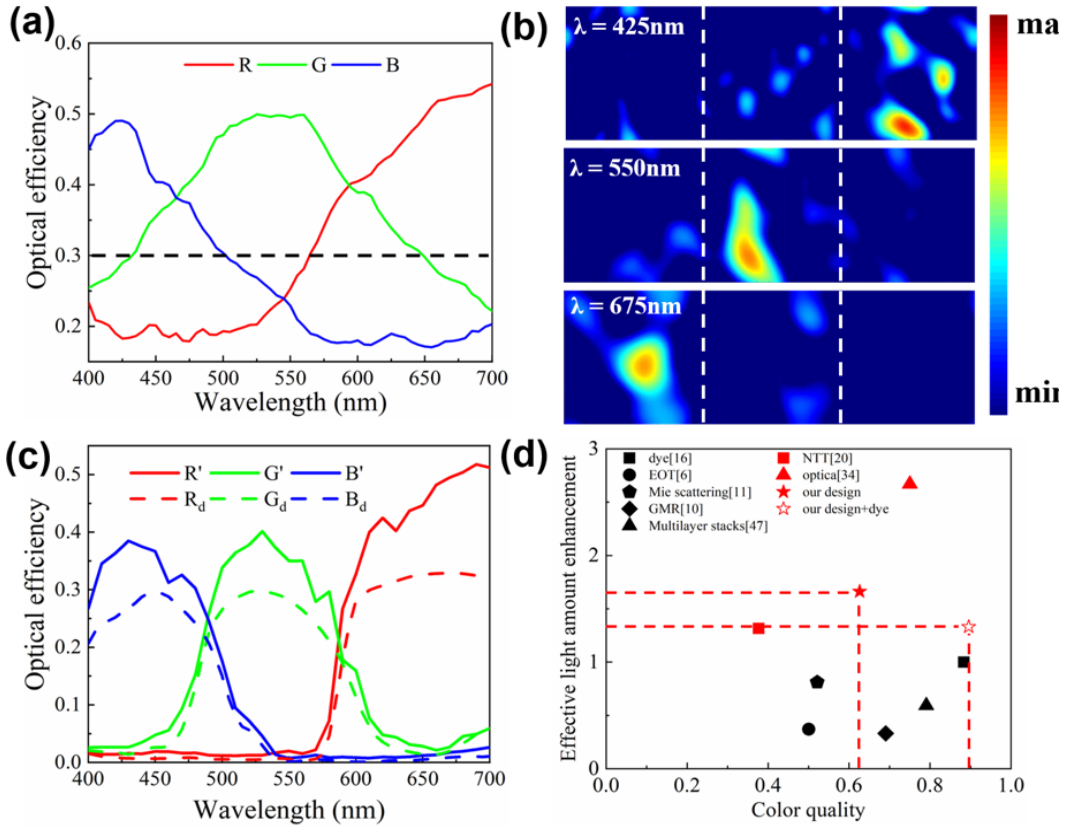

Figure 3. (a) Optical efficiencies of the nanorouter in *R*, *G* and *B* bands. Dashed line shows the average efficiency of current dye filtering technique. (b) Electric field distributions at the surface of silicon diodes at 425 nm, 550 nm and 675 nm. The spacer thickness is 4 μm. White dashed lines indicate the position of each pixel. (c) Optical efficiencies of the scheme combining nanorouters and dye filters. Dashed lines show the efficiencies of the scheme with only dye filters. (d) Comparison of the average color quality and the average effective light flux enhancement factor between various filters and routers with different mechanisms.

The optical efficiencies of the designed nanorouters are plotted in Figure 3a, where all three color bands show better performance than the average efficiency of current dye filtering technique indicated by the dashed line. The peak efficiencies of *R*, *G* and *B* pixels are all above 50% with an enhancement factor in a range of 1.63-1.81 times. The improvement of the signal-to-noise ratio encourages the further development of the current IS technique to sub-micron regions. Figure 3b shows the electric field distributions at the surface of silicon diodes at 425 nm, 550 nm and 675 nm, where light at three wavelengths concentrates to the expected pixels respectively. The results demonstrate the feasibility of the color nanorouters for efficient color sorting even for a multi-band requirement. Although the degeneration of optical efficiency is observed similar to the previously mentioned sectoring and

interleaving metasurfaces, the efficiency as high as 50% is still remarkable considering the current color filtering technique. An effective light flux enhancement factor is defined as the ratio of the collected light flux in the target color band to that of the dye filter scheme. As shown in Figure 3d, all the color filter schemes have small enhancement factors (<1). In particular, both EOT and GMR schemes have an average enhancement factor less than 0.4, where the EOT one suffers from its low transmission and the GMR one suffers from its narrowband resonance although it has high transmission. In contrast, all the color routing schemes show larger enhancement factors above 1. Although the EOT structure [31,32] and the multilayer stack [33] have been integrated in ISs and shown the expected color filtering function [2], the color routing schemes is more promising in terms of the optical efficiency. The best results are from the gradient based inverse design [24] with an enhancement factor of 2.67, where the feature size of 10 nm×10 nm and 3D randomly porous profile in a nanoscale require more effort in fabrication techniques. The proposed QR-cord like design is simple and has an average enhancement factor of 1.66, which is four times larger than the EOT scheme.

Apart from optical efficiency, color quality is another important performance specification. The color quality becomes zero when the detected color is close to a different primary color and it is equal to one if the detected color perfectly matches the indexed color. Actually, the color quality has been a bottleneck issue for the structural color technique especially in a transmissive configuration [4-9]. For example, the transmission and the linewidth are contractionary in metallic nanohole color filters based on the EOT effect [4]. The improvement of optical efficiency at a cost of large crosstalk is not expected. Generally, the dye filters based on the material absorption demonstrate sharp absorption edges to suppress the spectral crosstalk. Using such dye filters, the optical efficiencies of each pixel in a *R*-*G*-*B* unit cell is shown as dashed lines in Figure 3c. Assuming the *R*, *G* and *B* bands are 600nm-700nm, 500nm-600nm and 400nm-500nm, the spectral crosstalk is very small. As shown in Figure 3d, the average color quality of the *R*, *G* and *B* bands of the dye color filter scheme is as high as 0.88. In contrast, plasmonic color filtering techniques such as EOT phenomenon [4] usually have small average color qualities due to the broad resonance linewidth limited by the high absorption loss. Mie scattering filters also suffer from the low color qualities due to its scattering property [6]. Both two have an average color quality around 0.5. Metallic guided mode resonance (GMR) filters have less absorption loss due to its field concentration in the dielectric waveguide and thus provide a narrowband resonance resulting in an improved color quality

of 0.69 [11]. A large color quality of 0.79 can be obtained using multilayer stacks but the different stack structures of the *R*, *G* and *B* bands increase the complexity of fabrication [33]. In the single-pixel color deflector schemes demonstrated by Panasonic [22] and NTT [17], the designed *W*+*B* and *W*+*R* pixels inevitably induce flat profiles of the detected power spectra, which greatly increase the spectral crosstalk. For example, the NTT scheme has a color quality less than 0.4. The gradient based inverse design shows a large color quality of 0.75 due to the small limitation of the structure profile. The QR-code like scheme has a decent color quality of 0.63. There is one way to further reduce the spectral crosstalk of the QR-code like design for some applications with high requirements on the color quality. The dye color filters can be integrated underneath the nanorouters to filter out the crosstalk in each pixel and improve the color quality. In this case, the nanorouters can be integrated onto the current ISs without major modification of the standard processes. As shown in Figure 3c, the combined design with both dye color filters and nanorouters demonstrates three distinct spectra in *R*, *G* and *B* bands with small spectral crosstalk. At the same time, the optical efficiencies overcome the conventional dye color filters in all three bands. As seen from Figure 3d, in the combined structure the color quality increases to 0.9 with an average enhancement factor of 1.33. In addition, it is interesting to know the polarization dependence of the nanorouter considering the practical application [34]. It is found that the nanorouter can be engineered to be nearly insensitive to the polarization with a spectral correlation coefficients above 0.9 for a polarization angle in a range of 0-180° (Supporting information, S3).

Finally, it is interesting to predict the imaging performance with the full-color nanorouters. Although there is no experimental results, the actual imaging process can be modeled with a multispectral target image based on a conversion matrix method [17] as shown in Figure 4a. A multispectral image is selected from an open access website [35] as shown in Figure 4a. The reconstructed images with the *RGB* value obtained from an image sensor with dye filters and nanorouters (Supporting information, S4) are shown in Figure 4b and c respectively. Both images exhibit an excellent color quality with the original multispectral image. To visualize the difference in signal intensities of two schemes, the spectral integration of the collected flux in each pixel is linearly converted to gray values. The results of both dye filters and nanorouters are shown in Figure 4d and e respectively. It is obvious that the nanorouters scheme shows much larger signal intensity. Therefore, such a nanorouter integrated IS scheme with high optical efficiency and good color quality is promising for high resolution imaging application.

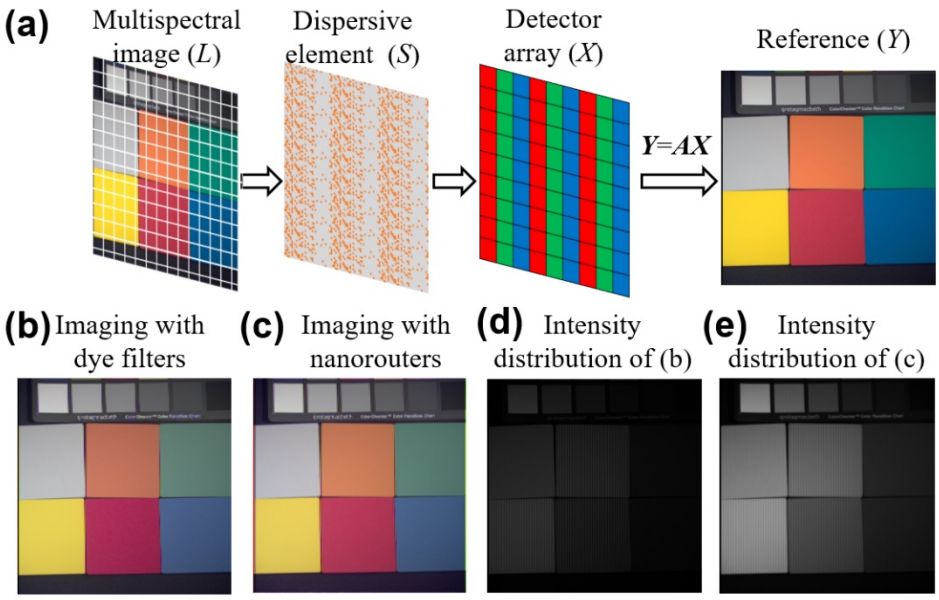

Figure 4. (a) Simulated imaging processes based on a multispectral image. (b) Reconstructed color image with dye filters ignoring the brightness. (c) Reconstructed color image with nanorouters in Fig. 3a ignoring the brightness. (d) and (e) are the grey-scale images of (b) and (c), respectively.

In conclusion, a QR-code like nanorouter is proposed for full-color routing in IS. Compared to various structure color techniques and the recently reported light routing techniques, the QR-code like nanorouter enables high optical efficiency with negligible color distortion in a simple structure, which is important for the development of low-cost ISs for high-resolution applications. The pixel level light routing function at multiple wavelengths overcomes various plasmonic and metasurface lenses. Over 60% signal enhancement is demonstrated in a 1.1 μm×1.1 μm pixel level compared to the state-of-the-art dye filter scheme. The proposed method is promising not only in ISs but also display and photovoltaics.

Acknowledgements

We are grateful for financial supports from National Key Research and Development Program of China (No. 2019YFB2203402), National Natural Science Foundation of China (Nos. 11774383, 92050108, 11774099, 11874029 and 11804120), Guangdong Science and Technology Program International Cooperation Program (2018A050506039), Guangdong Basic and Applied Basic Research Foundation (No. 2020B1515020037), Pearl River Talent Plan Program of Guangdong (No. 2019QN01X120). DRSC is supported by UK EPSRC Grant EP/T00097X/1.

The authors have declared no conflict of interest.

Data available on request from the authors

References

1. R. Fontaine, "The State-of-the-Art of Mainstream CMOS Image Sensors," in *International Image Sensors Workshop* (IISW) (2015), pp. 6-12.
2. Q. Chen, X. Hu, L. Wen, Y. Yu, D. R. S. Cumming, "Nanophotonic Image Sensors," Small **12**(36), 4922 (2016).
3. H. Rhodes, G. Agranov, C. Hong, U. Boettiger, R. Mauritzson, J. Ladd, I. Karasev, J. McKee, E. Jenkins, W. Quinlin, I. Patrick, J. Li, X. Fan, R. Panicacci, S. Smith, C. Mouli, J. Bruce, "CMOS imager technology shrinks and image performance," in *2004 IEEE Workshop on Microelectronics and Electron Devices* (2004), pp. 7-18.
4. Q. Chen, D. R. S. Cumming, "High transmission and low color cross-talk plasmonic color filters using triangular-lattice hole arrays in aluminum films," Opt. Express **18**(13), 14056-14062 (2010).
5. S. Song, X. Ma, M. Pu, X. Li, Y. Guo, P. Gao, X. Luo, "Tailoring active color rendering and multiband photodetection in a vanadium-dioxide-based metamaterial absorber," Photonics Research **6**(6), 492-497 (2018).
6. Y. Shen, V. Rinnerbauer, I. Wang, V. Stelmakh, J. D. Joannopoulos, M. Soljačić, "Structural colors from Fano resonances," ACS Photonics **2**(1), 27-32 (2015)
7. J. Berzins, S. Fasold, T. Pertsch, S. M. B. Bäumer, F. Setzpfandt, "Submicrometer nanostructure-based RGB filters for CMOS image sensors," ACS Photonics **6**(4), 1018-1025 (2019).
8. A. F. Kaplan, T. Xu, L. J. Guo, "High efficiency resonance-based spectrum filters with tunable transmission bandwidth fabricated using nanoimprint lithography," Appl. Phys. Lett. **99**(14), 143111 (2011).
9. Y. Yu, Q. Chen, L. Wen, X. Hu, H. F. Zhang, "Spatial optical crosstalk in CMOS image sensors integrated with plasmonic color filters," Opt. Express **23**(17), 21994-22003 (2015).
10. A. Kristensen, J. K. W. Yang, S. I. Bozhevolnyi, S. Link, P. Nordlander, N. J. Halas, N. A. Mortensen, "Plasmonic colour generation," Nat. Rev. Mater. **2**(1), 1-14 (2016).
11. P. Nagpal, N. C. Lindquist, S. H. Oh, D. J. Norris, "Ultrasmooth patterned metals for plasmonics and metamaterials," Science **325**(5940), 594-597 (2009).
12. Q. Chen, C. Martin, D. R. S. Cumming, "Transfer printing of nanoplasmonic devices onto flexible polymer substrates from a rigid stamp," Plasmonics **7**(4), 755-761 (2012).
13. H. Taguchi, M. Enokido, "Technology of Color Filter Materials for Image Sensor," in *International Image Sensor Workshop* (IISW) (2011), pp. 34-37.
14. Q. Chen, L. Liang, Q. Zheng, Y. Zhang, L. Wen, "On-chip readout plasmonic mid-IR gas sensor," Opto-Electron. Adv. **3**, 190040 (2020).
15. B. E. Bayer (Eastman Kodak Company), "Color imaging array," U.S. patent 3971065, (1976).
16. Y. Ye, Z. Liu, and T. Chen, "Toward transparent projection display: recent progress in frequency-selective scattering of RGB light based on metallic nanoparticle's localized surface plasmon resonance," Opto-Electron. Adv. **2**, 190020 (2019)
17. M. Miyata, M. Nakajima, T. Hashimoto, "High-sensitivity color imaging using pixel-scale color splitters based on dielectric metasurfaces," ACS Photonics **6**(6),

1442-1450 (2019).
18. T. Shegai, S. Chen, V. D. Miljković, G. Zengin, P. Johansson, M. Käll, "A bimetallic nanoantenna for directional colour routing," Nat. Commun. **2**(1), 1-6 (2011).
19. A. Nemati, Q. Wang, M. Hong, and J. Teng, "Tunable and reconfigurable metasurfaces and metadevices," Opto-Electron. Adv. **1**(5), 180009 (2018).
20. B. H. Chen, P. C. Wu, V. C. Su, Y. C. Lai, C. H. Chu, C. Lee, J. W. Chen, Y. H. Chen, Y. C. Lan, C. H. Kuan, D. P. Tsai, "GaN metalens for pixel-level full-color routing at visible light," Nano Lett. **17**(10), 6345-6352 (2017).
21. K. Dou, X. Xie, M. Pu, X. Li, X. Ma, C. Wang, and X. Luo, "Off-axis multi-wavelength dispersion controlling metalens for multi-color imaging," Opto-Electron. Adv. **3**(4), 190005 (2020).
22. S. Nishiwaki, T. Nakamura, M. Hiramoto, T. Fujii, and M. Suzuki, "Efficient colour splitters for high-pixel-density image sensors," Nat. Photonics **7**, 240-246 (2013).
23. D. Sell, J. Yang, S. Doshay, and J. A. Fan, "Periodic Dielectric Metasurfaces with High-Efficiency, Multiwavelength Functionalities," Adv. Opt. Mater. **5**(23), 1700645 (2017).
24. P. C. Muñoz, C. Ballew, G. Roberts, and A. Faraon, "Multifunctional volumetric meta-optics for color and polarization image sensors" Optica **7**(4), 280-283 (2020).
25. N. Zhao, P. B. Catrysse, and S. Fan, "Perfect RGB-IR Color Routers for Sub-Wavelength Size CMOS Image Sensor Pixels," Adv. Photonics Res. 2000048 (2021).
26. N. Srinivas and K. Deb, "Muiltiobjective Optimization Using Nondominated Sorting in Genetic Algorithms," Evolutionary Computation **2**(3), 221-248 (1994).
27. M. Khorasaninejad, W. T. Chen, R. C. Devlin, J. Oh, A. Y. Zhu, and F. Capasso, "Metalenses at visible wavelengths: Diffraction-limited focusing and subwavelength resolution imaging," Science **352**(6290), 1190-1194 (2016).
28. M. Khorasaninejad, A. Y. Zhu, C. R. Carmes, W. T. Chen, J. Oh, I. Mishra, R. C. Devlin, and F. Capasso, "Polarization-Insensitive Metalenses at Visible Wavelengths," Nano Lett. **16**(11), 7229-7234 (2016).
29. L. Lin, X. M. Goh, L. P. McGuinness, and A. Roberts, "Plasmonic Lenses Formed by Two-Dimensional Nanometric Cross-Shaped Aperture Arrays for Fresnel-Region Focusing," Nano Lett. **10**(5), 1936-1940 (2010).
30. Q. Chen, D. R. S. Cumming, "Visible light focusing demonstrated by plasmonic lenses based on nano-slits in an aluminum film," Opt. Express **18**(14), 14788-14793 (2010).
31. Q. Chen, D. Chitnis, K. Walls, T. D. Drysdale, S. Collins, and D. R. S. Cumming, "CMOS Photodetectors Integrated With Plasmonic Color Filters," IEEE Photonics Technology Letters **24**(3), 197-199 (2012).
32. Q. Chen, D. Das, D. Chitnis, K. Walls, T. D. Drysdale, S. Collins, and D. R. S. Cumming, "A CMOS Image Sensor Integrated with Plasmonic Colour Filters," Plasmonics **7**, 695-699 (2012).
33. L. Frey, P. Parrein, J. Raby, C. Pellé, D. Hérault, M. Marty, and J. Michailos, "Color filters including infrared cut-off integrated on CMOS image sensor," Opt. Express **19**(14), 13073-13080 (2011).

34. L. Wen, Q. Chen, X. Hu, H. Wang, L. Jin, and Q. Su, “Multifunctional Silicon Optoelectronics Integrated with Plasmonic Scattering Color,” ACS Nano **10**(12), 11076-11086 (2016).
35. F. Yasuma, T. Mitsunaga, D. Iso, and S.K. Nayar, “Generalized Assorted Pixel Camera: Post-Capture Control of Resolution, Dynamic Range and Spectrum,” Multispectral Image Database (2008), https://www1.cs.columbia.edu/CAVE/databases/multispectral/.